

### **MALAYSIAN JOURNAL OF ANALYTICAL SCIENCES**

Journal homepage: https://mjas.analis.com.my/



### Research Article

Scavenging aspirin using optimised date seeds based activated carbon via response surface methodology: Batch isotherm and bed column analysis

Md Mamoon Rashid, Erniza Mohd Johan Jaya, and Mohd Azmier Ahmad\*

School of Chemical Engineering, Engineering Campus, Universiti Sains Malaysia, 14300 Nibong Tebal, Penang, Malaysia

\*Corresponding author: chazmier@usm.my

Received: 6 May 2025; Revised: 4 August 2025; Accepted: 7 August 2025; Published: 31 October 2025

#### **Abstract**

Aspirin (ASP), which is commonly found in aquatic environments, presents notable risks to both ecosystems and human health. This investigation focuses on using an innovative adsorbent derived from date seeds, known as DSAC, to efficiently eliminate ASP from water. The preparation process was refined through response surface methodology (RSM), identifying ideal conditions at an activation time of 2.29 min, an activation power of 489 W, and a potassium hydroxide (KOH) impregnation ratio (IR) level of 1.63 g/g. Under these conditions, ASP removal was predicted at 76.58%, closely matched by an experimental value of 80.94%, with a minor deviation of 5.39%. The DSAC yield forecast was 26.22%, while the actual value reached 24.34%, marking a 7.72% difference. Analytical tests confirmed the suitability of DSAC, with a high BET surface area (BET-SA) of 1163.44 m²/g, a mesoporous surface area (MESO-SA) of 852.71 m²/g, a total pore volume (TPV) of 0.4899 cm³/g, and an average pore diameter (APD) of 2.94 nm. Isotherm analysis revealed that the adsorption system was best described by Langmuir, with a maximum uptake, Q<sub>m</sub> of 43.57 mg/g. In continuous column trials, optimal performance was observed when using a flow rate of 10 mL/min, an ASP concentration of 10 mg/L, and a column depth of 8 cm. These settings produced the longest durations before breakthrough and complete saturation, indicating superior adsorption performance. The findings highlight DSAC as a viable and environmentally friendly solution for treating pharmaceutical contaminants in water using fixed-bed systems.

Keywords: Activated carbon, adsorption, date seed, optimisation, isotherm, bed column

#### Introduction

The increasing use of medical treatments for humans and animals has led to pharmaceuticals becoming a major group of newly recognised pollutants in aquatic systems. These substances typically enter the environment due to the careless disposal of medications and the discharge of insufficiently treated wastewater from medical facilities, animal farming operations, and drug production sites [1]. Pharmaceutical pollution has become a major concern due to its harmful effects on aquatic life, human health, and surrounding ecosystems. Among anti-inflammatory these, nonsteroidal (NSAIDs) are widely used worldwide, with aspirin (ASP) being one of the earliest medications for managing pain, fever, and inflammation in both human and animals. Global ASP production and usage are estimated at 35,000 metric tons per year, with more than one trillion tablets consumed over the past century [2]. Because the human intestine does

not fully absorb many pharmaceuticals, as much as 90% of these substances can be eliminated via urine and faeces, eventually contributing to their presence in farm residues or being discharged into sewage systems [3]. Consequently, traces of ASP have been identified in water bodies across numerous nations [4]. Literature-based risk assessments indicate that ASP poses ecological hazards to aquatic systems. For instance, [5] reported that it induces oxidative stress and genetic damage in *Daphnia magna*. As a result, the ongoing environmental discharge of aspirin may lead to bioaccumulation in aquatic microbes, potentially transferring through the food web and endangering human health.

Multiple techniques have been investigated for removing pharmaceutical pollutants from wastewater. Among them, adsorption is particularly notable for its efficiency, relying on surface interactions and its wide suitability for trapping various types of contaminants such as textile dyes [6], pesticides [7], pharmaceutical residues [8], CO<sub>2</sub> gas [9], heavy metals [10] and so on. This method is favoured for its ease of application, high efficiency in eliminating pollutants, and overall affordability [11]. Activated carbon (AC) has historically been sourced from coal, a non-renewable material linked to environmental and financial issues. To promote sustainability, researchers increasingly are investigating agricultural by-products as viable alternatives such as rattan waste [12], biomass sludge [13], Alpinia galanga stem [14], oil palm empty fruit bunch [15], Tecoma chip waste [16] and others.

Several studies have explored the adsorption of aspirin using various biomass-derived activated carbons. For example, ASP adsorption onto spent tea leaves-based AC [17], tea waste extract-modified chitosan [18], and coffee waste-based AC [19]. However, these works predominantly use batch adsorption systems, which do not reflect the dynamic conditions of continuous flow processes in real wastewater treatment facilities. Furthermore, studies investigating fixed-bed column applications for ASP removal are extremely limited, and to the best of our knowledge, none have employed date seed-derived AC for this purpose. This study uniquely contributes by using date seed-derived AC, a sustainable and abundant biomass precursor, in fixed-bed column experiments for ASP removal.

Recent research has focused on improving AC production due to the many factors that affect its performance. Response surface methodology (RSM) is an advanced statistical approach that optimises multiple parameters simultaneously and provides precise modelling of the process [20]. Within the RSM, the central composite design (CCD) is preferred for reducing the number of experimental runs while capturing variable interactions and enabling accurate predictions. Three-dimensional (3D) response surface plots help visualise parameter effects, while model reliability and significance are assessed through ANOVA to ensure robust optimisation results [21]. This study used date seeds as a precursor for AC production, optimising conditions with RSM to enhance ASP adsorption from water. Chosen for their abundance in Saudi Arabia and natural strength, date seeds are typically discarded as waste. The research's novelty lies in evaluating continuous adsorption via a fixed-bed column, which is key for scaling up to real-world water treatment.

# Materials and Methods Precursor, chemicals, and gases

For this study, date seeds were collected from a local market in Abha, Saudi Arabia, and used as the primary precursor material for the synthesis of activated carbon. The powdered form of aspirin (ASP), with a purity of  $\geq$ 99.0%, and potassium hydroxide (KOH), with 90.00% purity, were sourced from Sigma-Aldrich. Additionally, high-purity nitrogen (N<sub>2</sub>) and carbon dioxide (CO<sub>2</sub>) gases, both with a purity of 99.99%, were supplied by MOX Gases Berhad, based in Malaysia.

#### **Synthesis of the DSAC**

The raw date seed precursor was initially washed thoroughly with tap water to remove surface impurities and any attached foreign materials. It was then subjected to oven drying at 60°C for 24 h to ensure complete moisture removal. After drying, the material was weighed and placed in a vertical furnace (Model Dwyer RMA-12-SSV, USA) for the carbonisation process. Pyrolysis was performed at 700°C for 3 h under a continuous flow of nitrogen (N<sub>2</sub>) gas to produce the char. This temperature was selected because pyrolysis at temperatures above 600°C is more effective for char formation. While the effect of the gaseous environment is negligible at 600°C, increasing the temperature to 750°C has been shown to enhance the pore volume and specific surface area, thereby improving the adsorption performance [22]. Therefore, 700°C was chosen as the optimal intermediate temperature for effective char production. This char was then activated using carbon dioxide (CO2) under various conditions, including microwave radiation times ranging from 2 to 6 min, radiation powers between 300 and 700 W, and KOH impregnation ratios (IR) varying from 0.50 to 2.50 g/g. The radiation power range of 300-700 W was also selected to optimise activation while minimising thermal degradation, as excessive power beyond 616 W can reduce the yield due to structural damage [23]. Similarly, a radiation time between 2 and 6 min was chosen because the date seeds had already undergone a carbonisation step. Prolonged exposure may rupture the pores, resulting in reduced adsorption capacity [21]. The optimisation of these activation parameters created a DSAC with enhanced properties. The specific experimental designs for the activation temperature, radiation time, and IR were developed using RSM, as outlined in Table 1. The IR was calculated using the following formula:

$$IR\left(\frac{g}{g}\right) = \frac{W_{KOH}(g)}{W_{char}(g)} \tag{1}$$

where  $W_{KOH}$  refers to the weight of KOH and  $W_{char}$  refers to the weight of the char.

### **Optimisation investigation**

To facilitate the optimisation process, the gathered data were carefully analysed using the sophisticated software Design Expert (Version 12), developed by STAT-EASE Inc. based in Minneapolis, USA. This software is specifically designed to perform advanced statistical analysis and process optimisation. The study focused on three key variables: radiation time (X1), radiation power (X2), and impregnation ratio (IR, X<sub>3</sub>). Additionally, two important responses were measured: the adsorption capacity for ASP (Y<sub>1</sub>) and the production yield of DSAC (Y2). Each of the variables was evaluated at three distinct coded levels: +1, 0, and -1, which represented radiation times of 2, 4, and 6 min, radiation powers of 300, 500, and 700 W, and IR values of 0.50, 1.50, and 2.50 g/g, respectively. The yield of DSAC was determined using the following formula:

$$Yield (\%) = \frac{W_{DSAC}}{W_p}$$
 (2)

where W<sub>DSAC</sub> is the dry mass of DSAC, and W<sub>p</sub> denotes the dry mass of the precursor.

### **Characterisation methods**

The physical and chemical properties of the prepared samples were comprehensively characterised, with a particular focus on evaluating the specific surface area using Brunauer-Emmett-Teller (BET) analysis, mesoporous structure, pore size distribution, and overall pore volume. These textural parameters were measured using the Micromeritics ASAP 2010 surface area and porosity analyser. To determine the elemental makeup, a Perkin Elmer Series II 2400 analyser from the United States was employed for precise elemental analysis. In addition, the surface structure and morphological details of the samples were closely examined using scanning electron microscopy (SEM), performed with the Quanta 450 FEG system manufactured in the Netherlands.

### Isotherm investigation

For the isotherm experiment, seven separate Erlenmeyer flasks were prepared, each filled with an ASP solution at different initial concentrations, C<sub>0</sub>: 5. 10, 15, 20, 30, 40, and 50 mg/L. These flasks were agitated under standardised laboratory conditions to ensure consistency. Each flask contained 200 mL of the ASP solution combined with 0.20 g of the optimised DSAC, and the temperature was consistently maintained at 30°C throughout the procedure. Once equilibrium was achieved, the residual concentration of ASP (Ce) in the solution determined using **UV-Visible** a spectrophotometer (Agilent Cary 60, USA). The UV-Vis spectrophotometer was calibrated with standard solutions before each measurement, and all experiments were conducted in triplicate with averaged values reported to ensure reproducibility. The number of ASP adsorbed at equilibrium, denoted as q<sub>e</sub> (mg/g), was calculated using the following equation:

$$q_e = \frac{(C_o - C_e)V}{W} \tag{3}$$

The experimental findings were analysed by applying a range of adsorption models, each described by its corresponding mathematical expression as detailed in the following:

Langmuir [24]:
$$q_e = \frac{Q_m K_L C_e}{1 + K_L C_e}$$
Freundlich [25]:
$$q_e = K_F C_e^{1/n_F}$$
Temkin [26]:

$$q_e = K_F C_e^{1/n_F} \tag{5}$$

$$q_e = \frac{RT}{B} \ln(AC_e) \tag{6}$$

The parameters related to each of these adsorption models are comprehensively explained in the work of [27].

# **Results and Discussion**

# Optimisation process: Regression model development

Table 1 summarises all experimental data, detailing the input factors and corresponding outcomes linked to DSAC synthesis optimised via RSM. The ASP adsorption capacity spanned from 47.88 to 95.30 mg/g, while the DSAC yield fluctuated between 14.40% and 29.40%. The software selected quadratic models to effectively predict the results. The equations for both the coded and actual factors are presented below:

ASP removal (%), 
$$Y_1$$
 (Actual values): 
$$Y_1 = -60.1812 + 27.4064X_1 + 0.21585X_2 + 41.97966X_3 - 0.00442X_1X_2 - 0.15X_1X_3 + 0.004912X_2X_3 - 3.29091X_1^2 - 0.000225X_2^2 - 13.99864X_3^2$$
 (7)

DSAC yield (%), 
$$Y_2$$
 (Actual values): 
$$Y_2 = 39.48 - 9.22X_1 - 0.0107X_2 + 8.97X_3 - 0.001125X_1X_2 - 0.1375X_1X_3 - 0.0035X_2X_3 + 0.9375X_1^2 + 0.000014X_2^2 - 1.95X_3^2$$
 (8)

ASP removal (%),  $Y_1$  (coded values):

$$Y_1 = 91.57 + 6.13X_1 + 3.19X_2 + 1.84X_3 + 1.77X_1X_2 - 0.30X_1X_3 + 0.9825X_2X_3 - 13.16X_1^2 - 9.00X_2^2 - 14.00X_3^2$$

$$(9)$$

DSAC yield (%),  $Y_2$  (coded values):

$$Y_2 = 19.05 - 4.98X_1 - 1.34X_2 + 0.82X_3 - 0.45X_1X_2 - 0.2750X_1X_3 - 0.70X_2X_3 + 3.75X_1^2 + 0.55X_2^2 - 1.95X_3^2$$
(10)

Table 1. Variables and responses for DSAC synthesis via RSM optimisation

	DSA	C Preparation Variable	es	Resp	onses
Run	Radiation Time, X <sub>1</sub> (min)	Radiation Power, X <sub>2</sub> (W)	IR, X <sub>3</sub> (g/g)	ASP Removal, Y <sub>1</sub>	DSAC Yield, Y <sub>2</sub> (%)
1	6 (+1)	500 (0)	1.5 (0)	89.15	16.10
2	6 (+1)	700 (+1)	2.5 (+1)	78.90	14.40
3	2 (-1)	700 (+1)	2.5 (+1)	55.14	25.90
4	2 (-1)	300 (-1)	2.5 (+1)	47.88	29.40
5	4(0)	500(0)	1.5(0)	93.90	18.80
6	4 (0)	500 (0)	1.5(0)	93.25	18.80
7	4(0)	500(0)	1.5(0)	92.45	18.40
8	6 (+1)	300 (-1)	0.5 (-1)	54.75	17.00
9	6 (+1)	700 (+1)	0.5 (-1)	55.80	14.50
10	4(0)	300 (-1)	1.5 (0)	81.50	21.50
11	4 (0)	500 (0)	1.5(0)	95.30	18.90
12	4 (0)	500 (0)	1.5(0)	91.40	18.80
13	4(0)	500 (0)	2.5 (+1)	85.00	17.50
14	4(0)	500 (0)	1.5 (0)	90.25	18.60
15	2 (-1)	300 (-1)	0.5 (-1)	49.23	29.30
16	4(0)	700 (+1)	1.5 (0)	86.40	17.50
17	4(0)	500 (0)	0.5 (-1)	72.56	16.50
18	2 (-1)	500 (0)	1.5 (0)	72.00	27.40
19	2 (-1)	700 (+1)	0.5 (-1)	51.10	25.60
20	6 (+1)	300 (-1)	2.5 (+1)	75.00	17.00

Figures 1(a) and 1(b) illustrate how closely the predicted results align with the actual measurements for ASP adsorption and DSAC output, respectively. For ASP, the coefficient of determination (R2) reached 0.9677, with an adjusted R2 of 0.9386. The DSAC yield followed with R2 at 0.9391 and adjusted R<sup>2</sup> at 0.8843, reflecting a strong correlation and excellent model accuracy in capturing response behaviour. The models also showed low variability, supported by standard deviation (S.D.) values of 4.23 for ASP and 1.47 for DSAC, suggesting consistent performance and minimal prediction Furthermore, adequate precision (A.P.) values stood at 14.99 for ASP and 14.07 for DSAC, well above the accepted threshold of 4, confirming reliable signal strength and strong predictive capabilities within the studied parameter range [28].

#### **Analysis of variance**

**Table 2** provides a detailed summary of the analysis of variance (ANOVA) findings for both ASP adsorption and DSAC production. The extremely low p-values, all below 0.0001, indicate that the models are statistically sound and highly dependable. These results affirm the strength, accuracy, and predictive validity of the developed models across the studied variables. [29]. In the case of ASP adsorption, the variables found to be statistically significant included X1, X2, X1², X2², and X3². For the DSAC yield, the analysis revealed that X1, X2, and X1² played key roles. Evaluation of the F-value showed that both ASP uptake and DSAC yield output were primarily affected by variations in irradiation time and power intensity.

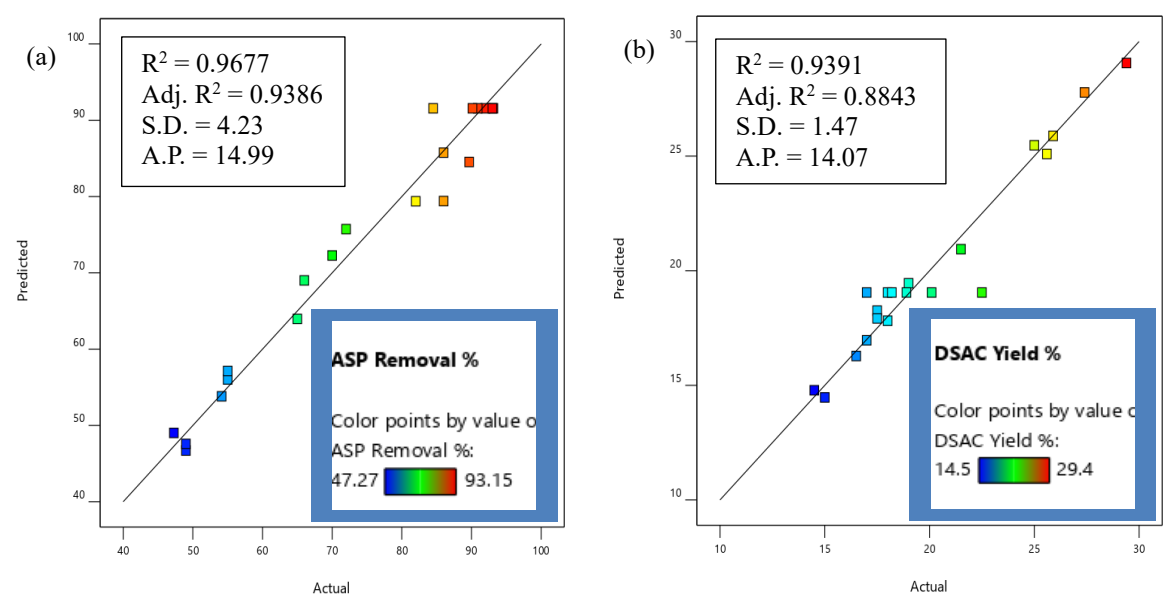


Figure 1. Estimated versus real plots for (a) ASP removal and (b) DSAC yield

Table 2. ANOVA results for ASP uptake and DSAC yield responses

Source	Response 1, Y1: ASP Uptake by DSAC								
Source	Sum of the Squares	DF	Mean Square	F-value	p-value				
Model	5367.47	9	596.39	33.28	< 0.0001				
$X_1$	375.40	1	375.40	20.95	0.0010				
$X_2$	101.51	1	101.51	5.66	0.0386				
$X_3$	33.86	1	33.86	1.89	0.1993				
$X_1X_2$	24.99	1	24.99	1.39	0.2650				
$X_1X_3$	0.7200	1	0.7200	0.0402	0.8452				
$X_2X_3$	7.72	1	7.72	0.4309	0.5264				
$X_1^2$	476.52	1	476.52	26.59	0.0004				
$X_2^2$	222.68	1	222.68	12.42	0.0055				
$X_3^2$	538.90	1	538.90	30.07	0.0003				

Source	Response 2, Y2: DSAC Yield								
Source	Sum of the Squares	DF	Mean Square	F-value	p-value				
Model	331.73	9	36.86	17.14	< 0.0001				
$X_1$	248.00	1	248.00	115.32	< 0.0001				
$X_2$	17.96	1	17.96	8.35	0.0161				
$X_3$	6.72	1	6.72	3.13	0.1075				
$X_1X_2$	1.62	1	1.62	0.7533	0.4058				
$X_1X_3$	0.6050	1	0.6050	0.2813	0.6074				
$X_2X_3$	3.92	1	3.92	1.82	0.2068				
$X_1^2$	38.67	1	38.67	17.98	0.0017				
$X_2^2$	0.8319	1	0.8319	0.3868	0.5479				
$X_3^2$	10.46	1	10.46	4.86	0.0520				

## Three-dimensional (3D) surface plot

To evaluate how microwave treatment influences the measured outcomes, three-dimensional (3D) response surfaces were constructed by adjusting both the radiation duration and power, while keeping the

IR fixed at 1.50 g/g. **Figure 2(a)** presents the response surface for the ASP removal efficiency, while **Figure 2(b)** displays the corresponding plot for the DSAC production. The peak ASP adsorption, recorded at 93.15%, occurred under conditions of

intensified radiation power at 550 W and extended exposure time of 5.00 min. The use of higher microwave energy facilitated the removal of volatile substances, which promoted pore formation and enlarged the surface area, ultimately enhancing the material's adsorption performance [30]. It also hastened the decomposition of light hydrocarbon compounds, leading to enhanced carbon formation and the development of a well-organised porous structure [31]. On the other hand, raising the radiation power beyond 550 W led to a noticeable decline in ASP adsorption, which was likely caused by pore collapse under intense microwave energy, which diminished the accessible surface area. Similarly, when the radiation duration exceeded 5.50 min, a continuous decrease in ASP uptake was observed, as excessive exposure damaged the pore architecture, thereby reducing the number of active sites available for adsorption [32].

As illustrated in **Figure 2(b)**, the maximum DSAC yield of 29.40% occurred under the lowest conditions studied, specifically at a radiation duration of 2.00 min and a microwave power setting of 300 W. A steady reduction in yield followed as both irradiation time and power were increased, with time extended to 6 min and power raised to 700 watts. This drop in yield is linked to intensified pyrolytic reactions

during microwave exposure, which caused substantial elemental depletion from the precursor material, ultimately lowering the carbon recovery [21]. Prolonged exposure to higher energy levels further accelerated this degradation pathway, leading to a continuous decline in DSAC production. Hence, the lowest yield, recorded at 14.50%, was observed under the most severe conditions of 6 min and 700 W.

### Optimal conditions and model validation

**Table 3** provides a summary of the optimised process conditions along with the validation of the model predictions. The optimisation approach targeted the minimal input variables and maximum response values. Based on the RSM analysis, the predicted optimal conditions were 2.29 min of radiation time, 489 W microwave power, and an IR of 1.63 g/g. Under these parameters, the model anticipated an ASP uptake of 76.58% and a DSAC yield of 26.22%. The experimental verification resulted in an ASP uptake of 80.94% and a DSAC yield of 24.34%, with respective error margins of 5.39% and 7.72%. The strong agreement between the predicted and experimental values, with deviations under 10%, highlights the accuracy and reliability of the developed models [33].

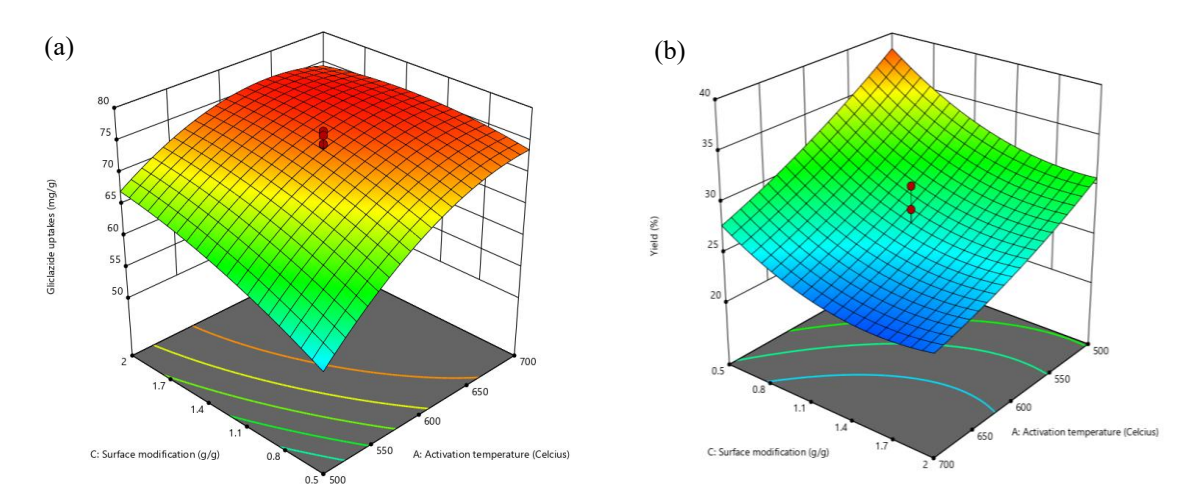


Figure 2. 3D surface plots for (a) ASP uptake and (b) DSAC yield responses

Table 3. Optimum conditions and model validation

Optimum Variables			Optimum Responses					
o p viii wii	. ,		ASP Uptakes, Y <sub>1</sub>			DSAC Yield, Y <sub>2</sub>		
X <sub>1</sub> (minutes)	X <sub>2</sub> (W)	X <sub>3</sub> (g/g)	Estimated (%)	Real (%)	Error (%)	Estimated (%)	Real (%)	Error (%)
2.29	489	1.63	76.58	80.94	5.39	26.22	24.34	7.72

 $\overline{X}_1$  = radiation time;  $X_2$  = radiation power;  $X_3$  = IR

### Characteristics of the samples Surface area and pore characteristics

**Table 4** outlines the textural and porosity properties of the starting material, carbonised sample, and the final DSAC product. Initially, the precursor exhibited limited porosity, as shown by its low BET surface area (BET-SA) of just 1.19 m<sup>2</sup>/g and a total pore volume (TPV) of only 0.0001 cm<sup>3</sup>/g. During carbonisation, pyrolytic reactions driven by the dehydration and volatilisation of light components, primarily derived from hemicellulose and cellulose, began forming initial pore structures. As a result, the char demonstrated notable increases across all measured parameters, including BET-SA, mesoporous surface area (MESO-SA), TPV, and average pore diameter (APD), which reached  $356.86 \,\mathrm{m}^2/\mathrm{g}$ ,  $0.2561 \,\mathrm{cm}^3/\mathrm{g}$ ,  $486.52 \text{ m}^2/\text{g}$ 2.75 nm, respectively. Additional porosity was introduced during the subsequent activation phase using KOH in combination with microwave heating. This process, particularly at higher power settings and longer exposure, enabled the breakdown of more complex volatiles, such as those arising from the hemicellulose-lignin networks. Concurrently, exposure to carbon dioxide encouraged further pore expansion and increased the porosity density. As a result, the optimised DSAC sample attained a marked improvement in its textural attributes, with a BET-SA of 1163.44 m<sup>2</sup>/g, MESO-SA of 852.71 m<sup>2</sup>/g, TPV of 0.4899 cm<sup>3</sup>/g, and an APD of 2.94 nm, a clear of a well-developed mesoporous indicator architecture. These enhancements underscore the synergistic role of KOH activation and CO2-assisted microwave treatment in tailoring the advanced porosity.

### Elemental and proximate analysis

**Table 5** presents a consolidated summary of the proximate and elemental compositions of the analysed samples. The date seed displayed a notably high fixed carbon content of 16.63%, which is greater than that found in other typical biomass materials such as rice husk (13.82%), corn straw (14.12%), and wood dust (14.46%), as reported by [34]. This elevated value supports the suitability of date seed as a precursor for DSAC production. Initially, the raw material had high levels of moisture and volatile matter, which were effectively reduced

to 2.31% and 23.63%, respectively, after undergoing carbonisation and chemical activation. Simultaneously, the fixed carbon content increased sharply to 71.57%. The resulting DSAC contained only 2.49% ash, a beneficial trait since ash does not contribute to the adsorption capacity, as noted by [35]. The elemental analysis showed similar trends. The carbon content increased from 45.21% in the untreated precursor to 78.35% in the processed DSAC. Meanwhile, the proportions of hydrogen, nitrogen, sulfur, and oxygen, elements typically associated with volatile compounds and moisture decreased due to thermal decomposition during the treatment process.

### Adsorption isotherm

Figure 3 shows the isotherm plots for the ASP-DSAC adsorption system at 30°C, while Table 6 presents a comprehensive summary of the parameters derived from fitting various isotherm models to the ASP-DSAC adsorption data. Among all the models tested, the Langmuir model showed the highest level of agreement with the experimental results, demonstrated by an excellent coefficient of determination, R<sup>2</sup> of 0.9928 and lowest root mean square error, RMSE of 0.85. This strong correlation suggests that adsorption likely occurs uniformly, with molecules forming a single layer on the surface of the adsorbent. The Langmuir model also assumes that all adsorption sites are energetically equivalent and that no significant interactions occur between the adsorbed molecules, which align well with the observed experimental trends. However, real wastewater systems often present heterogeneous surfaces and multi-component interactions, which may lead to deviations from ideal Langmuir behaviour. In such cases, multilayer adsorption or site heterogeneity could occur, which is better described by models such as Freundlich. Despite these limitations, the Langmuir model remains valuable for its ability to estimate the maximum monolayer adsorption capacity. In this study, the Langmuir model predicted a maximum adsorption capacity of 43.57 mg/g. The Freundlich constant, represented by n<sub>F</sub>, was found to be within the range of 1 to 10, reflecting a highly favourable adsorption environment.

 Table 4.
 Surface area and pore characteristics

Samples	BET-SA (m <sup>2</sup> /g)	MESO-SA (m²/g)	TPV (cm <sup>3</sup> /g)	APD (nm)
Precursor	1.19	-	0.0001	-
Char	486.52	356.86	0.2561	2.75
DSAC	1163.44	852.71	0.4899	2.94

Table 5. Elemental and proximate analysis of the samples

	Elemental Analysis (%)					Proximate Analysis (%)				
Samples	C	Н	N	S	*O+	Moisture	Volatile Matter	Fixed Carbon	Ash	
Precursor	45.21	6.82	1.56	0.17	46.24	6.35	75.45	16.63	1.57	
Char	69.53	5.11	1.44	0.14	23.78	5.46	49.52	43.50	1.52	
DSAC	78.35	4.19	1.25	0.1	16.11	2.31	23.63	71.57	2.49	

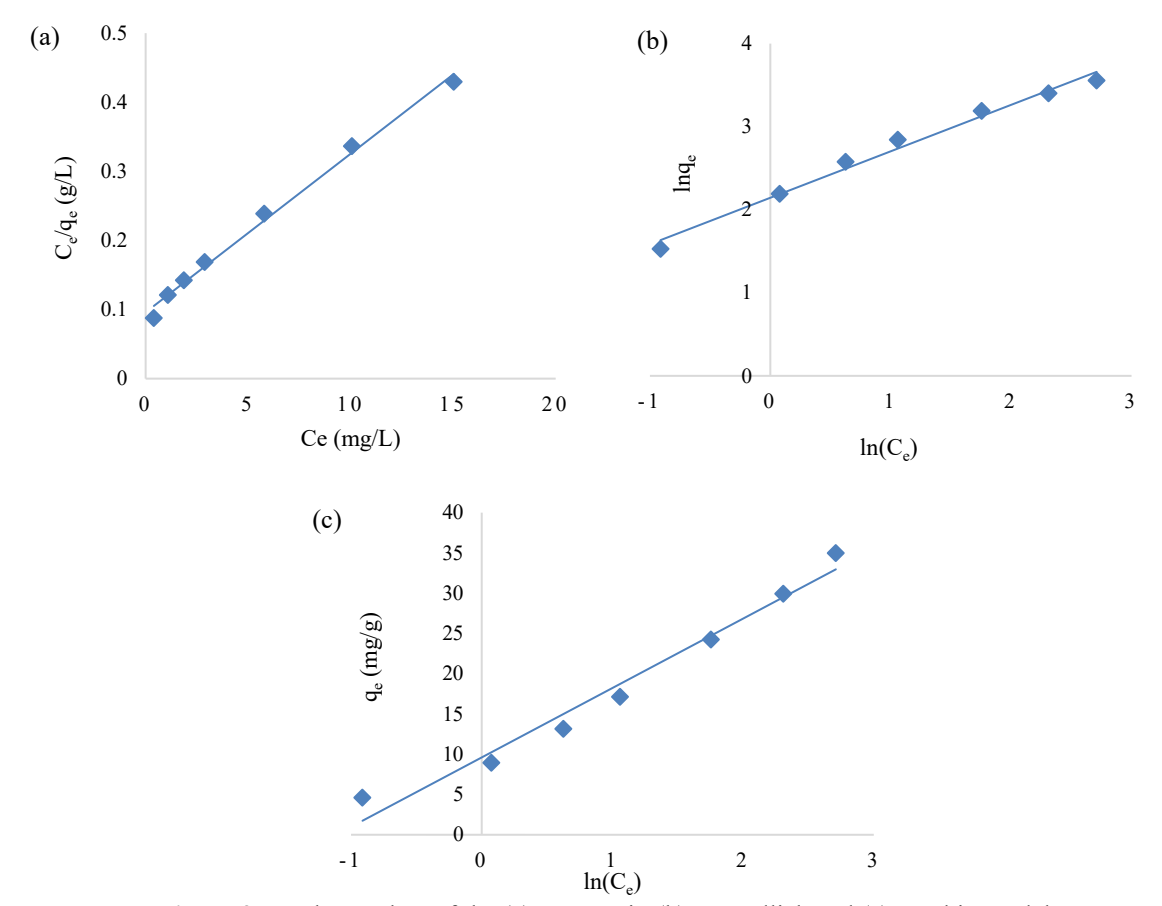


Figure 3. Isotherm plots of the (a) Langmuir, (b) Freundlich and (c) Temkin models

Table 6. Isotherm parameters for the ASP-DSAC adsorption system at 30°C

Langmuir	Values	Freundlich	Values	Temkin	Values
$Q_{\rm m}  ({\rm mg/g})$	43.57	$n_{\mathrm{F}}$	1.79	A <sub>T</sub> (L/mg)	8.62
$K_L(L/mg)$	0.2391	$K_F (mg/g)(L/mg)^{1/n}$	8.53	$B_T(L/mg)$	3.05
$\mathbb{R}^2$	0.9928	$\mathbb{R}^2$	0.9854	$\mathbb{R}^2$	0.9726
RMSE	0.85	RMSE	1.21	RMSE	1.76

### **Bed-column adsorption**

Bed column-based adsorption experiments played an essential role in assessing how the system functions in real-time operational settings. The study focused on three main aspects: how varying the flow rate influences performance, how different starting

concentrations affect outcomes, and how changes in the column height impact the process.

### Effect of the flow rate

The impact of varying flow rates on the adsorption of ASP by DSAC was investigated using values of 10, 20, 30, and 40 mL/min, with the column maintained

at a fixed bed height of 6 cm and an initial ASP concentration of 20 mg/L. As illustrated in Figure 4, increasing the flow rate resulted in a noticeable drop in the time required for breakthrough, which occurred around 30 min at the lowest rate and dropped to about 10 min at the highest rate. A similar trend was observed for the time to complete saturation, which decreased from approximately 80 min to approximately 27 min as the flow rate increased. Higher velocities caused the solution to pass through the adsorbent more quickly, reducing the opportunity for effective interaction and limiting the extent of adsorption. Conversely, slower flow conditions promoted longer contact between the solution and DSAC, enabling greater diffusion into the internal structure, more efficient site usage, and extended overall performance [2]. Out of all the flow rates examined, 10 mL/min proved to be the most effective, offering the greatest duration before breakthrough and full saturation occurred, which translated to superior adsorption performance.

### Effect of the initial concentration

Figure 5 presents the breakthrough profiles obtained for varying the starting concentrations of the adsorbate, specifically 10, 20, 30, and 40 mg/L, while keeping both the flow rate and bed height steady at 20 mL/min and 6 cm, respectively. As the concentration increased, the curves moved closer to the beginning of the time axis, revealing that the column reached saturation more quickly [36]. The breakthrough time declined from approximately 35 min at 10 mg/L to about 15 min at 40 mg/L, while complete saturation occurred at 80 min for the 10 mg/L and just 42 min for the 40 mg/L. Although higher concentrations created a stronger driving force for mass transfer, they also caused a more rapid depletion of the active sites [37]. Sharper curve slopes at elevated concentrations indicated swift saturation, whereas lower concentrations led to a more extended adsorption phase. Among all the conditions tested, 10 mg/L resulted in the most favourable performance, sustaining longer operation and greater uptake efficiency.

### Effect of the bed height

**Figure 6** illustrates the progression of breakthrough curves for ASP removal using different column depths of 2, 4, 6, and 8 cm, while keeping both the flow rate and initial concentration unchanged at 20 mL/min and 20 mg/L, respectively. As the column height increased, both the time to the initial breakthrough and the point of complete saturation were extended, suggesting improved uptake capacity. For the shallowest bed of 2 cm, breakthrough began around 13 min and full saturation followed at approximately 35 min. In contrast, the 8-cm column

delayed breakthrough until about 33 min and maintained adsorption until roughly 67 min. This enhancement at greater heights is likely due to the larger volume of the adsorbent material, which offered more surface area and prolonged interaction time with the solute. Shorter beds, having fewer active sites and shorter contact durations, reached saturation more quickly. Among all tested configurations, the tallest column provided the most effective performance, sustaining removal for the longest period and demonstrating the greatest adsorption efficiency.

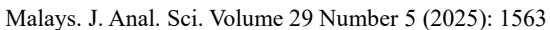
### **Breakthrough parameters**

Table 7 summarises the saturation time, total ASP adsorbed, and adsorption capacity of the fixed-bed column under different operational conditions. The saturation time shows how long the column can effectively remove ASP before the DSAC becomes saturated and ASP starts appearing in the outflow, while the total ASP adsorbed represents the absolute quantity of ASP removed. Adsorption capacity normalises uptake per gram of DSAC, allowing performance comparisons across varying bed masses.

At lower flow rates (10 mL/min), the column exhibited longer saturation (80 min) and higher adsorption efficiency (37.73 mg/g) because slower flow allowed extended contact time and greater diffusion of ASP into the DSAC pores. In contrast, higher flow rates (40 mL/min) reduced the contact time, leading to a quicker breakthrough (27 min) and lower total uptake (21.63 mg).

Increasing the initial concentration enhanced the total adsorption, from 16.14 mg at 10 mg/L to 33.64 mg at 40 mg/L, as the stronger concentration gradient provided a higher mass transfer driving force. The adsorption capacity also increased with the concentration, peaking at 79.22 mg/g, due to more complete utilisation of available active sites at higher solute loading.

For bed height, taller columns extended the saturation and increased the total ASP uptake, with the 8-cm bed achieving 32.01 mg, as more adsorbent provided additional surface area and longer diffusion pathways. However, the highest adsorption capacity (99.03 mg/g) was observed for the shortest bed (2 cm), reflecting the smaller adsorbent mass used for normalisation. These findings highlight importance of optimising flow rate, concentration, and bed height to maximise fixed-bed column performance. Table 8 summarises the comparison of DSAC's performance with other biomass-based adsorbents in adsorbing pharmaceuticals contaminants.



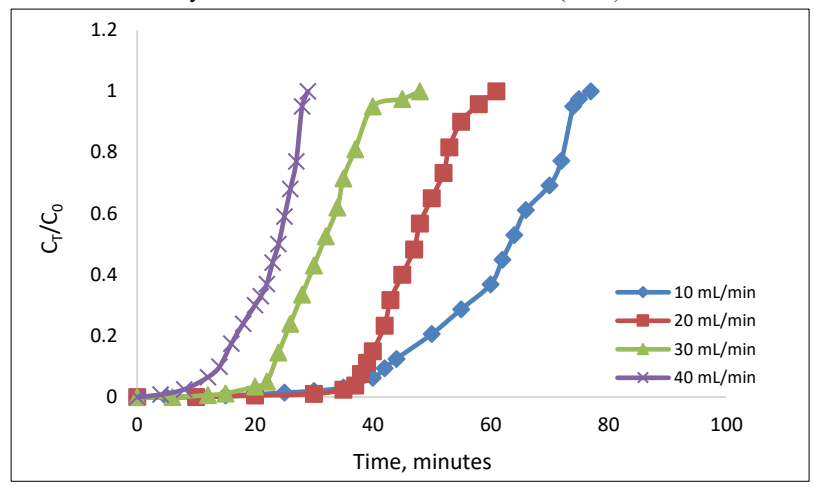


Figure 4. Breakthrough curve of the ASP-DSAC system at different flow rates

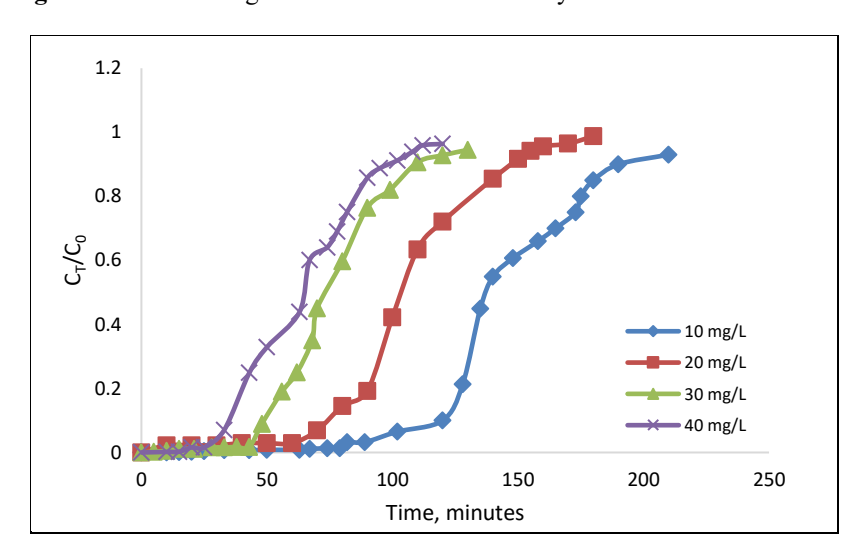


Figure 5. Breakthrough curve of the ASP-DSAC system at different initial concentrations

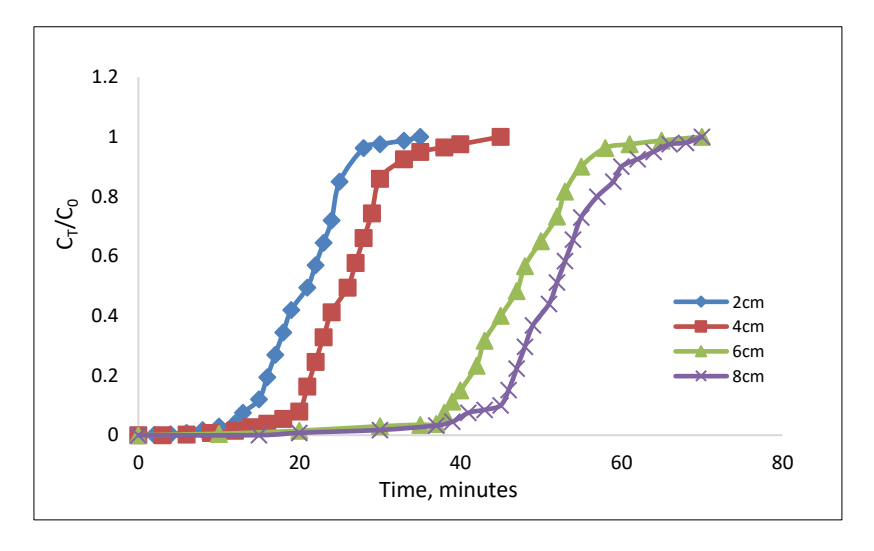


Figure 6. Breakthrough curve of the ASP-DSAC system at different bed heights

**Table 7**. Parameters for the ASP-DSAC breakthrough curve at different conditions

Conditions		Saturation Time (min)	Total ASP Adsorbed (mg)	Adsorption Capacity (mg/g)
	10	80	16.14	37.73
Elavarata (m.I./min)	20	60	24.37	56.59
Flow rate (mL/min)	30	40	24.72	56.59
	40	27	21.63	50.92
	10	80	16.14	37.73
I.::4:-1	20	70	28.05	66.0
Initial concentration (mg/L)	30	55	33.08	77.81
	40	42	33.64	79.22
	2	35	14.07	99.03
D- 41:-14 ()	4	50	20.71	70.73
Bed height (cm)	6	67	26.82	63.19
	8	80	32.01	56.59

Table 8. Comparison of DSAC's performance with other biomass-based adsorbents

Adsorbent	Adsorbate	BET-SA (m²/g)	Langmuir Adsorption Capacity, Qm (mg/g)	Bed Column Adsorption Capacity (mg/g)	Saturation Time (min)	Reference
DSAC	ASP	1163.44	43.57	99.03	80.00	This study
Tea waste extract— modified chitosan	ASP	-	-	63.60	85.00	[2]
Modified peanut shell	ASP	0.55	81.40	-	-	[38]
Cannabis sativum Hemp- based AC	Paracetamol	-	16.18	-	-	[39]
Malt bagasse-based biochar	Paracetamol	308.60	-	27.65	150.00	[40]
Acid-treated maize cob	Ibuprofen	7.92	36.81	-	-	[41]
Sunflower seed biochar	Ibuprofen	204.00	4.50	-	=	[42]

#### Conclusion

The date seed was first subjected to carbonisation at 700 °C for a duration of 3 h in a N2 atmosphere to obtain the base char. This material was then further enhanced using microwave-assisted activation in a CO<sub>2</sub> environment for 2.29 min at a power setting of 489 W, employing a KOH IR of 1.63 g/g, following the conditions recommended through optimisation. Under these settings, the predicted ASP removal reached 76.58%, while the experimental outcome was slightly higher at 80.94%, resulting in an error margin of just 5.39%. For the yield, the projected value was 26.22%, and the experimental yield was 24.34%, yielding a 7.72% difference. The regression outputs revealed strong agreement between the predicted and actual values, with R<sup>2</sup> of 0.9677 for ASP removal and 0.9391 for the DSAC yield.

Statistical analysis through ANOVA pointed to radiation duration and microwave power as the most

influential variables affecting both responses. The optimised DSAC showed a BET-SA of  $1163.44~\text{m}^2/\text{g}$ , MESO-SA of  $852.71~\text{m}^2/\text{g}$ , TPV of  $0.4899~\text{cm}^3/\text{g}$ , and an APD of 2.94~nm, all confirming the dominance of the mesoporous structure. The isotherm analysis aligned with the Langmuir model, yielding a  $Q_m$  of 43.57~mg/g. In the continuous flow experiments, the combination of a 10~mL/min flow rate, an initial concentration of 10~mg/L, and a column depth of 8~cm provided the longest operational times before breakthrough and full saturation, reflecting the best adsorption efficiency among the tested conditions. These findings support the promise of DSAC as an effective medium for fixed-bed adsorption systems.

#### Acknowledgement

This investigation is sponsored by the Malaysian Ministry of Higher Education under the Fundamental Research Grant Scheme (project code: FRGS/1/2023/TK05/USM/02/8).

#### References

- 1. Fernandes, J. P., Almeida, C. M. R., Salgado, M. A., Carvalho, M. F., and Mucha, A. P. (2021). Pharmaceutical compounds in aquatic environments occurrence, fate and bioremediation prospective. *Toxics*, 9(10): 257.
- Nordin, A. H., Ngadi, N., Nordin, M. L., Noralidin, N. A., Nabgan, W., Osman, A. Y., and Shaari, R. (2023). Spent tea waste extract as a green modifying agent of chitosan for aspirin adsorption: Fixed-bed column, modeling and toxicity studies. *International Journal of Biological Macromolecules*, 253: 126501.
- 3. Mohamad, F. M. Y., Abdullah, A. Z., and Ahmad, M. A. (2024). Amoxicillin adsorption from aqueous solution by Cu(II) modified lemon peel based activated carbon: Mass transfer simulation, surface area prediction and F-test on isotherm and kinetic models. *Powder Technology*, 438: 119589.
- Moghiseh, Z., Rezaee, A., Ghanati, F., and Esrafili, A. (2019). Metabolic activity and pathway study of aspirin biodegradation using a microbial electrochemical system supplied by an alternating current. *Chemosphere*, 232: 35-44.
- 5. Szabelak, A., and Bownik, A. (2021). Behavioral and physiological responses of Daphnia magna to salicylic acid. *Chemosphere*, 270: 128660.
- 6. Gunasekaran, S., Liu, A. J. X., and Ng, S. L. (2024). Activated carbon/iron oxide composites with different weight ratios for acid orange 7 removal. *Malaysian Journal of Analytical Sciences*, 28(6): 1359-1373.
- 7. Firdaus, M. Y. M., Rashid, M. M., Alam, M. M., and Ahmad, M. A. (2025). Copper-modified surface of orange peel-derived activated carbon for amoxicillin removal: Mass transfer simulation, attraction mechanism, and regeneration studies. *Arabian Journal for Science and Engineering*, 2025: 1-23.
- 8. Ramlee, D. A., Nordin, N. A., Rahman, N. A., and Bahruji, H. (2024). Removal of acetaminophen by using electrospun pan/sago lignin-based activated carbon nanofibers. *Malaysian Journal of Analytical Sciences*, 28(6): 1442-1457.
- Nur Syahirah Mohamed, H., Farihahusnah, H., Lai Ti, G., and Mohamed Kheireddine, A. (2024). Characterisation of egg whiteimpregnated activated carbon for CO<sub>2</sub> adsorption application. *Malaysian Journal of Science*, 43(Sp1): 20-25.
- 10. Khir, N. H. M., Salleh, N. F. M., Ghafar, N. A., Shukri, N. M., and Jusoh, R. (2025). Preparation and characterization of modified rambutan peels for the removal of chromium(VI) and nickel(II) from aqueous solution: Environmental impact

- and optimization *Malaysian Journal of Analytical Sciences*, 29(1): 1292.
- 11. Yusop, M. F. M., Ahmad, M. A., Rosli, N. A., Gonawan, F. N., and Abdullah, S. J. (2021). Scavenging malachite green dye from aqueous solution using durian peel based activated carbon. *Malaysian Journal of Fundamental and Applied Sciences*, 17(1): 95-103.
- Mohamad, F. M. Y., Rashid, M. M., Alam, M. M., and Ahmad, M. A. (2025). Copper metal-functionalized carbon from rattan waste via microwave pyrolysis for enhanced chloramphenicol removal: Optimization and F-test study. *Particuology*, 100: 196-213.
- Ahmad, M. A., Yusop, M. F. M., Awang, S., Yahaya, N. K. E. M., Rasyid, M. A. and Hassan, H. (2021). Carbonization of sludge biomass of water treatment plant using continuous screw type conveyer pyrolyzer for methylene blue removal. *IOP Conference Series: Earth and Environmental Science*, 765: 012112.
- Ahammad, N. A., Yusop, M. F. M., Mohd Din, A. T., and Ahmad, M. A. (2021). Preparation of alpinia galanga stem based activated carbon via single-step microwave irradiation for cationic dye removal. *Sains Malaysiana*, 50(8): 2251-2269.
- Ramli, F. F., Johar, A. N. M., Zabi, N., Mohamad, M., Hadzir, N. M., and Ibrahim, W. N. W. (2024). Sustainable sorbents: Oil palm empty fruit bunch-derived activated carbonalginate beads for organochlorine pesticides extraction in water samples. *Malaysian Journal* of Chemistry, 26(5): 583-597.
- Nasran, N. K. M., Firdaus, M. Y. M., Faizal, P. M. L. M., and Azmier, A. M. (2023). Alteration of Tecoma chip wood waste into microwave-irradiated activated carbon for amoxicillin removal: Optimization and batch studies. *Arabian Journal of Chemistry*, 16(10): 105110.
- Wong, S. L., Mohamed Noor, M. H., Ngadi, N., Mohammed Inuwa, I., Mat, R., and Saidina Amin, N. A. (2021). Aspirin adsorption onto activated carbon derived from spent tea leaves: statistical optimization and regeneration study. *International Journal of Environmental* Research, 15(2): 413-426.
- Nordin, A. H., Ngadi, N., Ilyas, R. A., Abd Latif, N. A. F., Nordin, M. L., Mohd Syukri, M. S., and Paiman, S. H. (2023). Green surface functionalization of chitosan with spent tea waste extract for the development of an efficient adsorbent for aspirin removal. *Environmental Science and Pollution Research*, 30(60): 125048-125065.
- 19. Boushara, R. S., Ngadi, N., Wong, S., and Mohamud, M. Y. (2022). Removal of aspirin from aqueous solution using phosphoric acid

- modified coffee waste adsorbent. *Materials Today: Proceedings*, 65: 2960-2969.
- Daouda, M. M. A., Akowanou, A. V. O., Mahunon, S. E. R., Adjinda, C. K., Aina, M. P., and Drogui, P. (2021). Optimal removal of diclofenac and amoxicillin by activated carbon prepared from coconut shell through response surface methodology. South African Journal of Chemical Engineering, 38(1): 78-89.
- Yusop, M. F. M., Baharudin, M. H., Rashid, M. M., Alam, M. M., and Ahmad, M. A. (2025). Amoxicillin adsorption onto oil palm trunk-derived activated carbon: synthesis optimization, modelling of mass transfer and ultrasonic regeneration. *Journal of Chemical Technology & Biotechnology*, 100(6): 1310-1327.
- Abdelaal, A., Benedetti, V., Villot, A., Patuzzi, F., Gerente, C., and Baratieri, M. (2023).
   Innovative pathways for the valorization of biomass gasification char: A systematic review. *Energies*, 16(10): 4175.
- 23. Firdaus, M. Y. M., Rashid, M. M., Alam, M. M., and Ahmad, M. A. (2025). Enhanced Cd<sup>2+</sup> removal via deprotonated-mango trunk functionalized carbon: Optimization and F-test for linear and non-linear isotherm and kinetic models. *Chemical Engineering Research and Design*, 220: 96-116.
- 24. Langmuir, I. (1918). The adsorption of gases on plane surfaces of glass, mica and platinum. *Journal of the American Chemical Society*, 40(9): 1361-1403.
- 25. Freundlich, H. (1906). Over the adsorption in solution. *Journal of Physical Chemistry*, 57(385471): 1100-1107.
- 26. Tempkin, M., and Pyzhev, V. (1940). Kinetics of ammonia synthesis on promoted iron catalyst. *Acta Physicochimica URSS*, 12(1): 327.
- Mohamad, F. M. Y., Abdullah, A. Z., and Ahmad, M. A. (2023). Adsorption of remazol brilliant blue R dye onto jackfruit peel based activated carbon: Optimization and simulation for mass transfer and surface area prediction. *Inorganic Chemistry Communications*, 158: 111721.
- 28. Beyan, S. M., Prabhu, S. V., Sissay, T. T., and Getahun, A. A. (2021). Sugarcane bagasse based activated carbon preparation and its adsorption efficacy on removal of BOD and COD from textile effluents: RSM based modeling, optimization and kinetic aspects. *Bioresource Technology Reports*, 14: 100664.
- Sopandi, T. P., Sulianto, A. A., Anugroho, F., Yusoff, M. Z. M., Mohamed, M. S., Farid, M. A. A., and Setyawan, H. Y. (2025). RSM-optimized biochar production from young coconut waste (*Cocos nucifera*): Multivariate analysis of nonlinear interactions between temperature, time,

- and activator concentration. *Industrial Crops and Products*, 223: 120157.
- 30. Yu, H., Mikšík, F., Thu, K., and Miyazaki, T. (2024). Characterization and optimization of pore structure and water adsorption capacity in pinecone-derived activated carbon by steam activation. *Powder Technology*, 431: 119084.
- 31. Weldekidan, H., Patel, H., Mohanty, A., and Misra, M. (2024). Synthesis of porous and activated carbon from lemon peel waste for CO<sub>2</sub> adsorption. *Carbon Capture Science & Technology*, 10: 100149.
- 32. Firdaus, M. Y. M., Nasran, M. N. K., Ridzuan, Z., Zuhairi, A. A., and Azmier, M. A. (2023). Mass transfer simulation on remazol brilliant blue R dye adsorption by optimized teak wood Based activated carbon. *Arabian Journal of Chemistry*, 16(6): 104780.
- Yusop, M. F. M., Mohd Johan Jaya, E., Mohd Din, A. T., Bello, O. S., and Ahmad, M. A. (2022). Single-stage optimized microwave-induced activated carbon from coconut shell for cadmium adsorption. *Chemical Engineering & Technology*, 45(11): 1943-1951.
- 34. Wei, X., Huang, S., Yang, J., Liu, P., Li, X., Wu, Y., and Wu, S. (2023). Adsorption of phenol from aqueous solution on activated carbons prepared from antibiotic mycelial residues and traditional biomass. *Fuel Processing Technology*, 242: 107663.
- Aziz, A., Mohamad Yusop, M. F., and Ahmad, M. A. (2024). Harnessing microwave energy to transform *Nephelium lappaceum* L. peel into activated carbon for chloramphenicol eradication in aqueous solutions. *Materials Chemistry and Physics*, 318: 129311.
- 36. Patel, H. (2019). Fixed-bed column adsorption study: A comprehensive review. *Applied Water Science*, 9(3): 45.
- 37. Gupta, A., and Garg, A. (2019). Adsorption and oxidation of ciprofloxacin in a fixed bed column using activated sludge derived activated carbon. *Journal of Environmental Management*, 250: 109474.
- Zhang, X., Han, X., Liu, Y., Han, R., Wang, R., and Qu, L. (2023). Remediation of water tainted with noxious aspirin and fluoride ion using UiO-66-NH<sub>2</sub> loaded peanut shell. *Environmental Science and Pollution Research*, 30(41): 93877-93891.
- 39. Sajid, M., Bari, S., Saif Ur Rehman, M., Ashfaq, M., Guoliang, Y., and Mustafa, G. (2022). Adsorption characteristics of paracetamol removal onto activated carbon prepared from *Cannabis sativum* Hemp. *Alexandria Engineering Journal*, 61(9): 7203-7212.
- 40. Silveira Neto, A. L., Pimentel-Almeida, W., Niero, G., Wanderlind, E. H., Radetski, C. M.,

- and Almerindo, G. I. (2023). Application of a biochar produced from malt bagasse as a residue of brewery industry in fixed-bed column adsorption of paracetamol. *Chemical Engineering Research and Design*, 194: 779-786.
- 41. Thabede, P. M. (2024). The adsorption of Ibuprofen from aqueous solution using acid treated maize cob. *Case Studies in Chemical and Environmental Engineering*, 9: 100718.
- 42. Alvear-Daza, J. J., Cánneva, A., Donadelli, J. A., Manrique-Holguín, M., Rengifo-Herrera, J. A., and Pizzio, L. R. (2023). Removal of diclofenac and ibuprofen on mesoporous activated carbon from agro-industrial wastes prepared by optimized synthesis employing a central composite design. *Biomass Conversion and Biorefinery*, 13(14): 13197-13219.